ciated flow reversal, takes place. The same results were found for the other steady flow situations investigated.

Wake formation was also observed above the upper part of the steam heated cylinder. The surface of the cylinder was approximately isothermal, due to the condensation of steam on the interior wall. The Grashof number based on the cylinder diameter was 1×10^{10}. The steady state flow patterns were identical to those discussed above for the other geometry.

During transient flow periods for the geometry shown in Fig. 1, very irregular flow separation and reversal were seen near the center of the upper part of the surface for short periods. Figure 3 shows such a regime. Stagnation points are seen near the centerline of the surface and are similar to the kind of flow reversal which appears in a forced flow separated by unfavorable pressure gradients. However, this separation during the transient period is thought to be generated by the incoming leading edge effects. No such reversals were observed after the starting transient. Since there was no noticeable fluid circulation or stratification in the tank during the short experiment, it is not thought that the observed separation was caused by peculiar conditions in the tank.

The above observations suggest that the usual expression "flow separation" is not an appropriate term for natural convection flows. The suggested mechanism is apparently not in operation as a flow turns away from the surface under increasing action of a component of the buoyancy force normal to it. Of course the flow must separate as two opposed buoyancy generated layers from opposite sides of a surface meet at the top. But the impetus for this, the pressure field which changes their direction, is generated in the flow layers and immediately adjacent to the surface, not in an external region.

ACKNOWLEDGEMENTS

The authors wish to acknowledge support from the National Science Foundation under Research Grant GK-18529 for this research. The first author wishes to acknowledge support as a graduate research assistant from the same grant.

REFERENCES

1. H. J. MERK and J. A. PRINS, Thermal convection in laminar boundary layers, I, II, III, *Appl. Sci. Res.* **4A**, 11–24, 195–206, 207–224 (1953–1954).
2. R. J. BROMHAM and Y. R. MAYHEW, Free convection from a sphere in air, *Int. J. Heat Mass Transfer* , 83–84 (1962).
3. A. A. KRANSE and J. SCHENK, Thermal free convection from a solid sphere, *Appl. Sci. Res.* **19A**, 397–403 (1965).
4. J. SCHENK and F. A. A. SCHENKELS. Thermal free convection from an ice sphere in water, *Appl. Sci. Res.* **19**, 465–476 (1968).
5. K. T. YANG, Laminar free-convection wake above a heated vertical plate, *J. Appl. Mech.* **31**, 131–138 (1964).

Int. J. Heat Mass Transfer. Vol. 15, pp. 177–180. Pergamon Press 1972. Printed in Great Britain

A NOTE ON THE TURBULENT SCHMIDT AND LEWIS NUMBERS IN A BOUNDARY LAYER

R. L. SIMPSON and R. L. FIELD

Department of Mechanical Engineering, Southern Methodist University, Dallas, Texas 75222, U.S.A.

(*Received* 18 *August* 1970 *and in revised form* 10 *May* 1971)

NOMENCLATURE

D_1, molecular mass diffusion coefficient of component 1 into component 2, $\dot{m}_1'' = -D_1 \rho \frac{\partial Z_1}{\partial y}$ [m²/s];

$\frac{k}{U_\infty}$, $\frac{\dot{m}_{1w}''}{\rho_\infty U_\infty (Z_w - Z_\infty)}$, mass diffusion coefficient, [dimensionless];

Le_t, $\frac{Pr_t}{Sc_t}$, turbulent Lewis number [dimensionless];

$\dot{m}_1''$, mass flux of component 1 into component 2 [kg/m²s];

Pr_t, $\frac{\varepsilon_M}{\varepsilon_H}$, turbulent Prandtl number [dimensionless];

Sc, $\frac{\nu}{D_1}$, molecular Schmidt number, [dimensionless];

Sc_t, $\frac{\varepsilon_M}{\varepsilon_D}$, turbulent Schmidt number, [dimensionless];
U, mean velocity in the main-stream direction [m/s];
V, mean velocity perpendicular to the surface [m/s];
x, distance along the plate in the flow direction [m];
y, perpendicular distance from the surface [m];
Z, mole fraction of helium;
$\bar{Z}$, $\frac{Z - Z_w}{Z_\infty - Z_w}$, dimensionless concentration ratio;
Γ, $\int_0^\infty \frac{U}{U_\infty}\left[\frac{Z - Z_\infty}{Z_w - Z_\infty}\right] dy$, mass concentration thickness [m];
ε_D, eddy mass species diffusivity [m^2/s];
ε_H, eddy thermal diffusivity [m^2/s];
ε_M, eddy viscosity [m^2/s];
δ, boundary layer thickness, y where $U/U_\infty = 0.99$ [m];
ν, kinematic viscosity [m^2/s];
ρ, density [kg/m^3].

Subscripts
t, denotes turbulent contribution;
w, indicates wall condition;
∞, denotes free-stream condition.

INTRODUCTION

IN A RECENT issue of this journal, Simpson, Whitten and Moffat [1] presented experimental results for the distribution of the turbulent Prandtl number in an air boundary layer with injection and suction. No foreign gases were considered in that study. However, in the more general case of foreign gas injection, the turbulent Schmidt number distribution must be known in order to determine the mass transfer from the relation

$$\frac{\dot{m}_1''}{\rho} = -\left(\frac{\nu}{Sc} + \frac{\varepsilon_M}{Sc_t}\right)\frac{\partial Z_1}{\partial y}. \quad (1)$$

The purposes of this note are to provide some experimental information on the turbulent Schmidt number distribution of an external boundary layer, since no other direct work is known, and to point out the relationship between the turbulent Schmidt and Prandtl numbers, i.e. the turbulent Lewis number.

COMPUTATION OF THE TURBULENT SCHMIDT NUMBER

The mass-transfer coefficient and velocity and concentration profile data of Kendall [2], and his reevaluated friction factor results [3], were used in the turbulent Prandtl number computing method described by Simpson, Whitten, and Moffat [1] to compute the turbulent Schmidt number distribution in a constant free-stream velocity boundary layer. Kendall's data are for injection of small concentrations of helium ($Sc = 0.211$) into a constant free-stream velocity turbulent flow of air through a flat porous wall. The concentration of helium at the wall varied from 0·12 to 0·39 per cent. An uncertainty of ± 0.005 per cent was reported for the helium concentrations [2]. The free-stream velocity was nominally 50 fps, with the mass flux ratio ($\rho_w V_w/\rho_\infty U_\infty$) nominally 0·0001, 0·001, 0·003 and 0·005. Profiles with the smallest longitudinal wall concentration gradient (dZ_w/dx) and free-stream velocity gradient were selected so that the non-dimensional concentration profile similarity could be used in the computing method.

The method of Simpson *et al.* [1] is valid for determining the turbulent Schmidt number from experimental data if the non-dimensionalized mass concentration is substituted for the non-dimensional temperature, the mass transfer coefficient for the Stanton number, and the mass concentration thickness for the enthalpy thickness. However, one addition to this scheme is required to determine Sc_t. The data of Simpson, Whitten, and Moffat [1] were taken with a negligible wall temperature gradient in the x direction. Thus the dT_w/dx term in the integral energy equation could be neglected in [1] in determining Pr_t. However, the variation with respect to x in test wall helium concentration could not be neglected in the case of Kendall's data. Therefore, to determine Sc_t for the data of Kendall, the integral mass concentration equation must to be considered in the form [3]

$$\frac{d\Gamma}{dx} = \frac{-\Gamma}{(Z_w - Z_\infty)}\frac{d(Z_w - Z_\infty)}{dx} + \frac{k}{U_\infty} + \frac{\rho_w V_w}{\rho_\infty U_\infty}. \quad (2)$$

The first term on the right of equation (2) (term 1) was between 1 and 17 per cent (see Fig. 1) of $d\Gamma/dx$ in all cases studied. For a given concentration profile, the Sc_t results obtained without this term were about the same percentage higher than the results obtained considering this term.

DISCUSSION AND CONCLUSIONS

Figure 1 presents Sc_t vs. y/δ results obtained by considering all the terms of equation (2). No systematic variation with x is observed. The shape of the band of data is similar to the Pr_t distribution of [1] for an external turbulent boundary layer. Very close to the wall ($y/\delta < 0.1$) the results are relatively uncertain and diverge into scatter as do the Pr_t results of [1], due partly to uncertainties in locating the probes relative to the wall and partly to the small turbulent transport relative to the total contribution. In the outer region, $Sc_t < 1$ like Pr_t, although $Sc_t \to 0$ as $y/\delta \to 1$ while Pr_t results were divergent at the outer edge of the boundary layer. Unlike Pr_t, Sc_t in the outer region is slightly dependent on the blowing mass flux ratio, being on the average slightly higher with higher blowing rates. This small difference between the Pr_t results of [1] and these Sc_t results is attributed to the fact that Kendall's reevaluated $C_f/2$ results were slightly lower [4] than the $C_f/2$ results used in [1] for the same flow conditions.

The empirical curve of Rotta [5] for Pr_t, shown on Fig. 1,

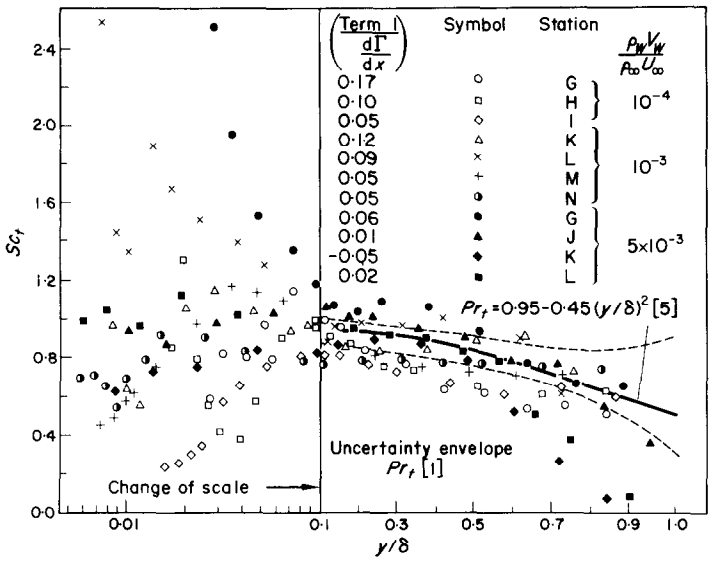

FIG. 1. Experimental results from the data of Kendall [2], Sc_t vs. y/δ.

closely fits the data of [1] in the outer region and can be used as an approximation for Pr_t. This distribution was used in computing the turbulent Lewis number (Pr_t/Sc_t) results shown on Fig. 2 for $y/\delta > 0{\cdot}2$. For $y/\delta < 0{\cdot}2$, the experimental Pr_t of [1] were used. Le_t based on the results shown in Fig. 1 is smaller than when based on Sc_t results obtained without term 1. Even though the uncertainty in these results is rather large, it appears that the normal assumption that $Le_t = 1$ in the outer region is supported by these results.

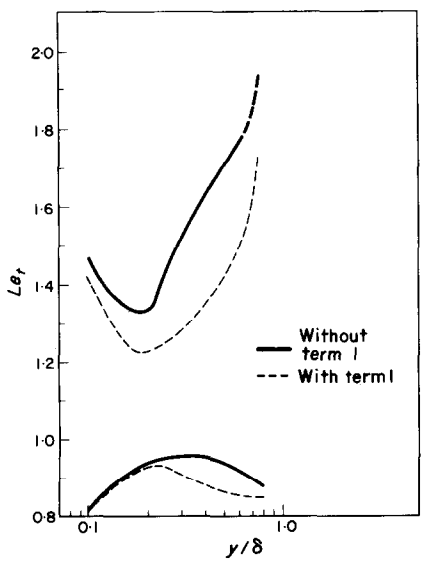

FIG. 2. Le_t vs. y/δ, data scatter envelopes for experimental results from the data of Simpson *et al.* [1] and Kendall [2].

Several conclusions can be made from these results. The Sc_t and Pr_t distribution in the outer region of an external turbulent boundary layer are closely the same and therefore indicate $Le_t = 1$ in the outer region of the boundary layer where turbulent processes dominate transport. Furthermore, $Sc_t < 1$ and $Pr_t < 1$ in the outer region even though $Sc = 0{\cdot}211$ and $Pr = 0{\cdot}72$, a trend indicating that even with $Sc = Pr = 1$ the Pr_t and Sc_t are not likely to be unity in this outer region.

These experimentally derived conclusions support the outer region hypothesis of [1] and others [1]: that the diffusion of heat and other scalars such as mass species and turbulent energy is a combination of gradient and large eddy transport while the transport of mainstream momentum, a vector quantity, is a velocity gradient process associated with small scale turbulence. Hence, effective ε_D or ε_H values representing the same combined gradient and large eddy transport mechanisms would be the same and would be greater than the gradient transport alone, yielding $Pr_t = Sc_t < 1$ and $Le_t = 1$, even if $Sc = Pr = 1$.

REFERENCES

1. R. L. SIMPSON, D. G. WHITTEN and R. J. MOFFAT, An experimental study of the turbulent Prandtl number of

air with injection and suction, *Int. J. Heat Mass Transfer* **13**, 125–143 (1970).
2. R. M. KENDALL, Interaction of mass and momentum transfer in the turbulent boundary layer, Sc.D. thesis, M.I.T. (1959).
3. R. M. KENDALL, M. W. RUBESIN, T. J. DAHM and M. R. MENDENHALL, Mass, momentum and heat transfer within a turbulent boundary layer with foreign gas mass transfer at the surface. Part 1: Constant fluid properties, Vidya, Report 111, Palo Alto, Cal., DDC No. AD 619 209 (Feb. 1964).
4. R. L. SIMPSON, R. J. MOFFAT and W. M. KAYS, The turbulent boundary layer on a porous plate: Experimental skin friction with variable injection and suction, *Int. J. Heat Mass Transfer* **12**, 771–789 (1969).
5. J. C. ROTTA, Temperturverteilungen in der Turbulenten Grenzschicht an der Ebenen Platte, *Int. J. Heat Mass Transfer* **7**, 215–228 (1964).

Int. J. Heat Mass Transfer. Vol. 15, pp. 180–184. Pergamon Press 1972. Printed in Great Britain

GENERALIZED HEAT TRANSFER AND FRICTION CORRELATIONS FOR TUBES WITH REPEATED-RIB ROUGHNESS

R. L. WEBB
The Trahe Company, La Crosse, Wisconsin, U.S.A.

E. R. G. ECKERT and R. J. GOLDSTEIN
The University of Minnesota, Minneapolis, Minnesota, U.S.A.

(*Received* 24 *May* 1971)

NOMENCLATURE

D, pipe inside diameter (to base of rib);
D_{eq}, pipe equivalent diameter ($D - e$);
D'_{eq}, defined by Hall [8];
e, rib height;
e^+, roughness Reynolds number, $e^+ \equiv eu^*/\nu = (e/D)Re\sqrt{(f/2)}$;
f, rough tube friction factor, $(\Delta P/L)\, D/2\rho u_m^2$;
$\bar{f}$, rough tube % friction factor based on D_{eq};
$\bar{g}$, $[(f/2St - 1)/\sqrt{(f/2)} + u_e^+]Pr^{-0.57}$ (repeated-ribs);
p, distance between repeated-ribs;
Pr, Prandtl number;
Re, Reynolds number, Du_m/ν;
$\bar{Re}$, Reynolds number based on D_{eq};
St, rough tube Stanton number;
u, local fluid velocity;
u_m, average fluid velocity;
u^*, friction velocity, $\sqrt{(\tau_0/\rho)}$;
u_e^+, $\sqrt{(2/f)} + 2{\cdot}5 \ln(2e/D) + 3{\cdot}75$;
$\tilde{u}_e^+$, $\sqrt{(2/f)} + 2{\cdot}5 \ln[2e/(D - e)] + 3{\cdot}75$;
y, coordinate distance normal to surface;
τ_0, apparent wall shear stress, $(D/4)(dP/dx)$.

INTRODUCTION

IN A PREVIOUS publication [1] correlations are presented for the friction factor and Stanton number of "repeated-rib" roughness in turbulent pipe flow. Figure 1 shows a sketch of this geometry and defines the roughness parameters as p/e and e/D; two dimensionless parameters should be sufficient,

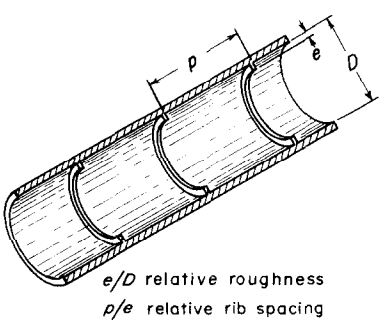

FIG. 1. Sketch of the roughness geometry.